Template-Free Electrochemical Synthesis of Superhydrophilic Polypyrrole Nanofiber Network

Jianfeng Zang,[†,‡] Chang Ming Li,*[,†] Shu-Juan Bao,[†] Xiaoqiang Cui,[†] Qiaoliang Bao,[†] and Chang Q. Sun[‡]

School of Chemical and Biomedical Engineering and Center for Advanced Bionanosystems, Nanyang Technological University, 70 Nanyang Drive, Singapore 637457, and School of Electrical & Electronic Engineering, Nanyang Technological University, 50 Nanyang Avenue, Singapore 639798

Received June 15, 2008; Revised Manuscript Received July 26, 2008

ABSTRACT: In this work, a superhydrophilic polypyrrole (PPy) nanofiber network is electrochemically synthesized in an aqueous solution by using phosphate buffer solution (PBS) in the absence of templates, surfactants and structure-directing molecules. FESEM, X-ray diffraction, UV−visible absorption, and contact angle measurement were employed to characterize the nanofiber network. The effect of synthetic conditions including pH, oxidation potential and concentrations of phosphate, pyrrole (Py) and dopant ClO_4^- on the PPy nanostructure is systematically investigated. A mechanism for the nanofiber formation in an aqueous solution without assistance of any "hard" and "soft" template is proposed, in which the presence of the hydrogen bonding between phosphate and Py oligomers is essential to producing the 1D nanofiber structure, and the electrostatic interactions between ion dopant and Py oligomers lead to an irregular nanostructure. This is a simple, environmentally friendly and one-step approach to fabricate a PPy film with unique nanostructure and chem-physical properties, which can have great potential in various applications such as sensors, electronics, and energy source systems.

Introduction

Conductive polymers (CPs) with one-dimensional (1D) nanostructures such as nanofibers, nanotubes and nanorods have been used as molecular building blocks to construct nanoelectronic devices,[1] field-effect transistors,[2] sensors[3] and actuators.[4] The straightforward approach toward 1D nanostructures is to confine the chemical or electrochemical oxidation of monomers in a porous "hard template" such as zeolites,[5] alumina,[6] and tract-etched polymeric membranes.[7] An alternative popular route employs a structure-directing molecule such as surfactant,[8] organic acid,[9] DNA,[10] and polyelectrolyte[11] as a "soft template" or "molecule template". The main disadvantage of the "soft" and "hard" template-assisted synthesis is that it is tedious and expensive due to its involvement of multiple, complicated steps or the post-treatment process. Recently, polyaniline nanofibers have been templatelessly synthesized through either dilute-chemical[12] polymerizations or interfacial polymerizations.[13] However, either the approach is still time-consuming or an organic, nonenvironmentally friendly solvent is needed during the interfacial synthesis. Further, the formation mechanism of 1D CPs via such a template-free approach remains unclear. Therefore, it would be of both scientific and technological interest to explore a simple, economic and reliable route for synthesis of nanostructured CPs in an aqueous solution with a controlled manner, which in turn can provide broad applications.

Polypyrrole (PPy) is one of the most important CPs because of its high stability, electronic conductivity, ion exchange capacity and biocompatibility. Various PPy including its derivatives, nanoarrays and nanocomposites have been synthesized for different promising applications.[14,15] 1D nanostructured PPy has also been synthesized by using "hard" templates[16] and "soft" templates such as organic acids,[15] surfactants[17] and ionic liquid.[18] In this work, a simple, economic and environmentally friendly approach is investigated to fabricate PPy nanofibers, a 1D nanostructure, by using phosphate buffer solution (PBS) without any "hard" or "soft" template. The hydrophilicity of the synthesized PPy nanofiber network, which is essential in their sensing and biomedical applications, is studied by water contact angle measurements. The driving forces in formation of the PPy nanofiber assisted by a "soft" template are often attributed to hydrophobic interaction, electrostatic interaction and/or hydrogen bonding between the polymer molecule and the templates.[19] The templateless synthesis of the polyaniline nanofibers with using organic solvents is ascribed to the separation of nucleation and elongation processes or the suppression of the second growth of the polymer.[13,20] To explore the formation mechanism of 1D PPy nanofiber in an aqueous solution, without using the organic solvent, we systematically investigate the effects of various synthetic conditions including pH, oxidation potential and concentrations of PBS, pyrrole (Py) and dopant ClO_4^- on the produced PPy nanostructures. X-ray diffraction (XRD) and UV−vis absorption are used to examine the nanostructured PPy for the mechanism analysis. Based on the experimental results, a new mechanism is proposed for the template-free synthesis of 1D nanostructured PPy in an aqueous solution.

Experimental Section

Materials. All chemicals were purchased from Aldrich and were of analytical grade except additional description. Py was distilled under reduced pressure. A series of phosphate buffer solutions (PBSs) with various pH values were prepared by adjusting the molar ratio of $[Na_2HPO_4]/[NaH_2PO_4]$ and dilution of 1 M PBS with deionized water.

Preparation of PPy Nanofiber. The PPy nanofiber was potentiostatically polymerized at 0.85 V vs Ag/AgCl with a CHI-660B electrochemical station (CH Instruments Inc. USA) in an aqueous solution with pH 6.8 containing 0.1 M Py, 0.07 M $LiClO_4$ and 0.2 M PBS, if no additional description. A 300 nm thin gold film deposited on silicon wafer with an intermediate layer of Ti was used as the working electrode, and a platinum sheet and Ag/AgCl were used as the counter and reference electrode, respectively. Irregular structured PPy was prepared with 0.1 M Py and 0.07 M $LiClO_4$.

Characterization. The morphologies of the produced PPy films were investigated with a field-emission scanning electron microscope (FESEM, JSM-6700F, JEOL, Japan), and their element

* Corresponding author. E-mail: ecmli@ntu.edu.sg. Tel: +65-67904485. Fax: +65-67911761.
† School of Chemical and Biomedical Engineering and Center for Advanced Bionanosystems.
‡ School of Electrical & Electronic Engineering.

10.1021/ma801345k CCC: $40.75
Published on Web 09/04/2008

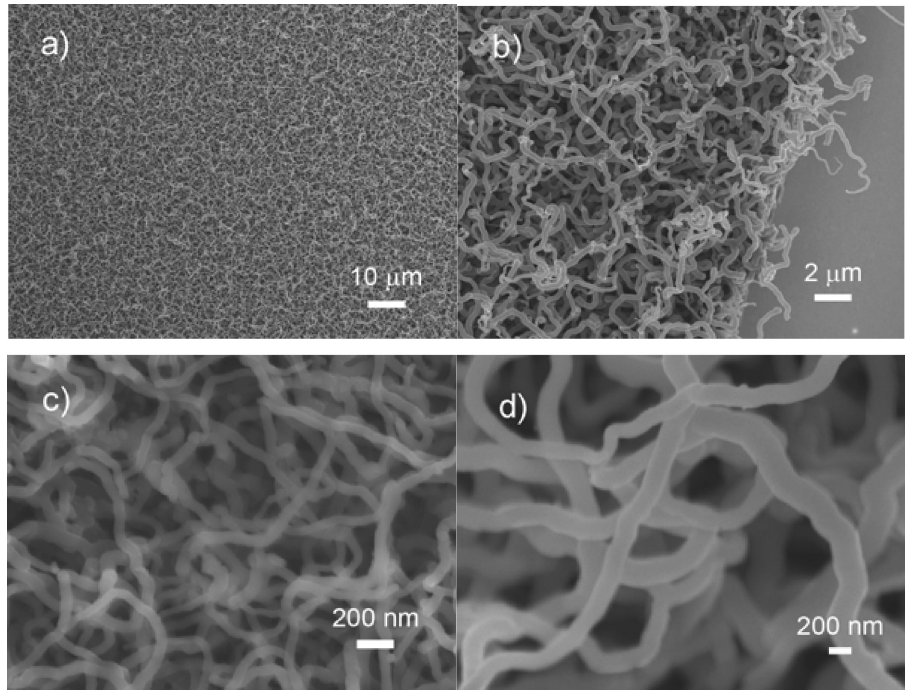

Figure 1. FESEM images of PPy nanofiber network. (a) Low magnification image and (b) edge view of the PPy nanofiber network. High magnification images of PPy nanofiber network formed at (c) 120 s and (d) 1 h.

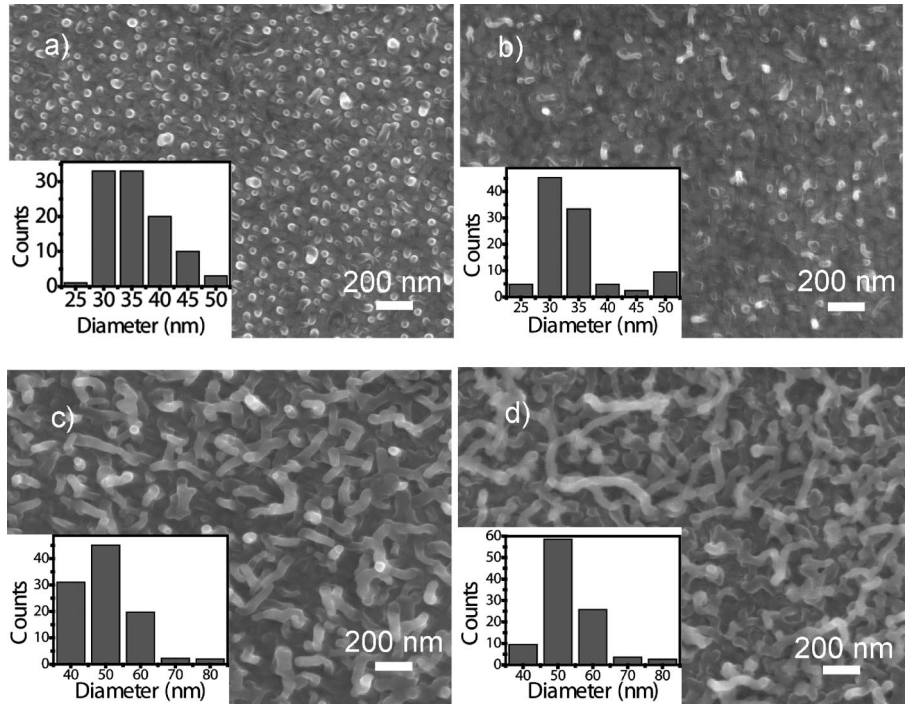

Figure 2. PPy nanofiber formed at different growth stages. The deposition time is (a) 1, (b) 5, (c) 10 and (d) 30 s.

analysis was conducted by energy dispersive X-ray (EDX). The XRD pattern was obtained with an XRD instrument (Bruker AXS X-ray diffractionmeter, Germany). The absorption spectra of PPy were recorded by a UV−visible spectrophotometer (Shimadzu UV-2450, Japan) with a resolution at 1 nm. Contact angles (CAs) were measured with FTA200 system (First Ten Angstroms, Inc., USA) at ambient temperature.

Results and Discussion

As shown in Figure 1, a homogeneous PPy nanofiber network is potentiostatically synthesized at a large scale without assistance of any "hard" or "soft" template. The diameters of the nanofibers are in a range of 50−220 nm, and can be simply controlled by the reaction time from 2 min (Figure 1c) to 1 h (Figure 1d). The formation process of the PPy nanofiber structure was investigated from infant to its growth. Many small nanorods with diameters of 25−50 nm are formed within 1 s of reaction time (Figure 2a), which grows larger and longer in 5 s (Figure 2b). After 10 s of reaction time, the 1D PPy nanofibers are clearly formed (Figure 2c) with heads perpendicular to the substrate surface. With further growth until 30 s,

the nanofibers become even longer and larger with diameters in a range of 40−80 nm (Figure 2d). A PPy nanofiber network is finally produced after 2 min (Figure 1c). Compared to the original sizes of the nanorods at 1 s, the length of the nanofiber increases at least 3 orders of magnitude, while the radius of the fiber only enlarged 1 order of magnitude. This indicates that the elongation growth rate is much faster than that in the radial direction, thus resulting in a fiber instead of nanoparticles.

The effects of the synthetic conditions including pH, oxidation potential and concentrations of PBS, Py and ClO_4^- on the nanostructure of the PPy fibers were studied. In each experiment only one condition was the variable but the ratio of $[HPO_4^{2-}]/[H_2PO_4^-]$ was kept constant for pH 6.8 through change of total phosphate concentration, i.e. $[PBS] = [HPO_4^{2-}] + [H_2PO_4^-]$. Experimental results demonstrate that only irregular shaped PPy forms at a phosphate concentration smaller than 0.05 M (Figure S1a in the Supporting Information). A microrod PPy with a diameter around 2 μm starts to occur after PBS is up to 0.1 M (Figure S1b in the Supporting Information). When PBS is over 0.2 M, the PPy nanofiber forms (Figure S1c in the Supporting Information). Particularly, when PBS was zero in the solution, only irregular shaped PPy was generated, no matter how we changed other parameters. The results here clearly reveal that PBS involves the reaction to form 1D nanostructure and a minimum PBS concentration is required. The pH value was changed by adjusting the ratio of $[HPO_4^{2-}]/[H_2PO_4^-]$ while keeping the total concentration of phosphate constant (PBS 0.2 M). An irregular shaped PPy (Figure S2a in the Supporting Information) and the microrod PPy with diameter of 1−2 μm (Figures S2b and S2c in the Supporting Information) form, respectively when pH is 6.0 and 6.4−6.6. However, the 1D nanofiber PPy is produced when pH is above 6.8 (Figure S2d in the Supporting Information). The result shows that a high pH promotes the nanofiber formation process. A control experiment was conducted and further confirmed that PPy nanofiber could be formed through HPO_4^{2-} in the solution free of $H_2PO_4^-$ (Figure S2e in the Supporting Information). The effect of Py concentration on the PPy nanostructure (Figures S3a and S3b in the Supporting Information) shows that irregular PPy forms at a Py concentration >0.1 M (Figures S3a and S3b in the Supporting Information) while the nanofiber is produced at a Py concentration ≤0.1 M (Figure S3c in the Supporting Information). The concentration of ClO_4^- also has considerable effect on the produced PPy nanostructure. When ClO_4^- concentration is ≥0.2 M and ≤0.07 M, irregular shaped PPy (Figure S4a in the Supporting Information) and nanofiber PPy (Figures S4c and S4d in the Supporting Information) form, respectively. It is observed that microrod PPy begins to form when ClO_4^- achieves 0.1 M (Figure S4b in the Supporting Information). The existence of the dopant ClO_4^- was confirmed with EDX analysis. The nature of the deposition potential is actually related to the electrochemical polymerization rate. A high polymerization potential would cause fast deposition of PPy. Results show that the microrod PPy starts to form at an oxidation potential ≥0.95 V (Figure S5a in the Supporting Information), but only nanofiber is produced when the potential range is over 0.65−0.85 V (Figure S5b in the Supporting Information). In a brief, the experimental results above demonstrate that the presence of PBS is the most critical factor among all influential synthesis conditions to produce the PPy nanofiber structure, and a relatively high concentration of PBS (≥0.2 M), high pH (≥6.8), low concentration of Py (≤0.1 M), low concentration of dopant ClO_4^- (≤0.07 M) and low oxidation potential (≤0.85 V) favor the formation of 1D PPy nanofiber.

Based on the experimental observations above, a mechanism for the template-free formation of the PPy nanofiber in an aqueous solution is proposed as shown in Scheme 1. It is known

Scheme 1. Schematic Illustration of the Proposed Mechanism for the Template-Free Formation of PPy Nanofiber in an Aqueous Solution[a]

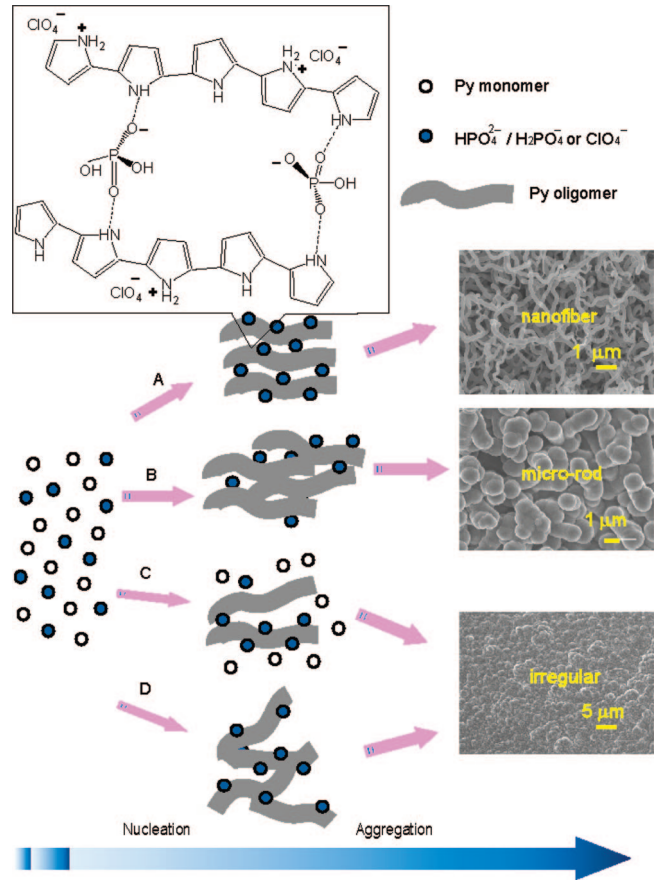

[a] (A) Nanofiber forms when experimental conditions favor the self-alignment of the oligomers by hydrogen bonding. (B) Microrod forms when the random aggregation process is comparable to the self-alignment process. (C) Irregular shaped PPy forms when the electrochemical reaction rate is much faster than the diffusion rate of the self-aligned Py oligomers or the self-alignment rate of Py oligomers. (D) Irregular shaped product forms when the random aggregation process dominates. The inset is hydrogen bonds formed between the oligomers and $HPO_4^{2-}/H_2PO_4^-$.

that Py can form various oligomers and further randomly aggregate or orderly self-assemble, strongly depending on the nature of its interaction with the anion present and/or the surface of the electrode,[21] in which electrostatic interactions enhance the random aggregation, while hydrogen bonding promotes the oligomer orderly self-alignment.[22] In the PBS/Py system presented here, electrostatic interactions occur between the electrooxidized, positively charged Py/oligomers and anions, while the hydrogen bonding is produced by the N−H group of the Py ring and the oxygen atoms of the phosphate anion. Thus, during the nucleation process, if the solution environment favors hydrogen bonding to complex Py and $HPO_4^{2-}/H_2PO_4^-$, the oligomers could self-align to form a well-ordered bundle structure (Scheme 1A). Clearly, the ordered oligomer bundles can serve as seeds to result in further growth of the 1D PPy nanostructures for the template-free formation process. That is why a minimum of PBS concentration is required to produce the nanofibers (Figure S1c in the Supporting Information). The pH effect can be explained since a high pH environment dissociates H^+ of $HPO_4^{2-}/H_2PO_4^-$ to promote its complex with Py through hydrogen bonds (Figure S2d in the Supporting Information). In contrast, if the electrostatic reaction is much stronger than the hydrogen bond, it would break the self-aligned

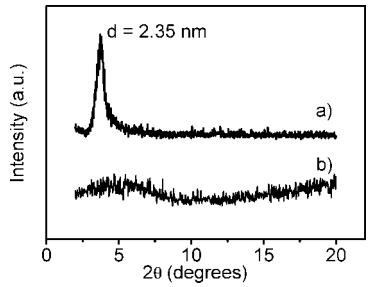

Figure 3. XRD patterns of (a) PPy nanofiber and (b) irregular shaped PPy.

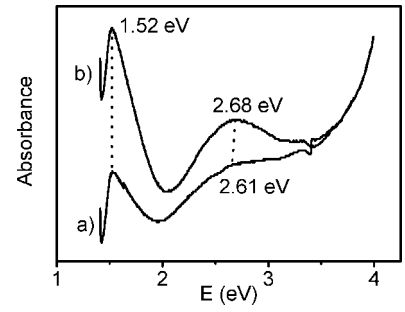

Figure 4. The UV−vis absorption spectra of (a) PPy nanofiber and (b) irregular shaped PPy.

Py oligomer for random aggregation, resulting in irregular shapes (Scheme 1D). A strong acid has a weak conjugate base including hydrogen bond. $HClO_4$ is a strong acid, and thus the role of ClO_4^- is mainly an anionic dopant through its strong ionic bonds rather than its weak hydrogen bonds in the PPy polymerization. Since electrostatic interactions enhance the random aggregation,[21] a high concentration of ClO_4^- should produce irregular PPy nanostructure, which is well in agreement with the results illustrated above (Figure S4a in the Supporting Information). However, when the random aggregation rate is comparable to the self-alignment, it possibly results in microrods with diameters in a micron scale (Scheme 1B). It is also discovered that, for all cases, the formation mechanism of PPy electrodeposition involves the simultaneous presence of adsorption and 3D nucleation, limited by diffusion of Py and/or different Py oligomer species in the processes.[23] If the electrochemical reaction rate is much faster than the diffusion rate of the self-aligned Py oligomers or the self-alignment rate of Py oligomers (in solution or on electrode surface), only Py could diffuse onto the electrode surface and thus an irregular PPy structure could be produced as shown in Scheme 1C. The rate of an electrochemical reaction can be boosted by a high polymerization potential and a high reactant concentration. Thus, irregular nanostructure formation at a high oxidation potential or a high concentration Py (Figures S3a and S3b in the Supporting Information; Figures S5a and S5b in the Supporting Information) is in good agreement with the mechanism proposed in Scheme 1C.

Using the proposed mechanism we can also explain the formation of the nanofiber network. As shown in Scheme 1A, HPO_4^{2-} is likely to play the major role in formation of the ordered-bundle structure and further developed network compared to $H_2PO_4^-$. In comparison to $H_2PO_4^-$, HPO_4^{2-} has a higher charge/volume ratio to form stronger hydrogen bonding. Increase of both phosphate concentration and pH value results in the increase of $[HPO_4^{2-}]$; therefore the conditions are favorable for ordered-bundle network structure formation and for further developed nanofiber network at the end.

The existence of the well-ordered bundle structures of the polymer chains in PPy nanofiber is supported by the low angle XRD result (Figure 3). An intense peak at $2\theta = 3.76°$ is shown in the XRD pattern of the nanofiber (Figure 3a), which is not observed in irregular shaped PPy (Figure 3b). The corresponding Bragg spacing $d = 2.35$ nm is assigned as the periodic distance of the aligned PPy chains, indicating the existence of supermolecular order in the PPy nanofiber network.[16,24] In contrast, only a broad weak hump is observed in the XRD pattern of irregular shaped PPy (Figure 3b). This shows that no short-range ordered structure of polymer chains is in the irregular shaped product.

The UV−vis spectrum of PPy nanofiber indicates the existence of hydrogen bonds (Figure 4). The absorption spectrum of PPy nanofiber (Figure 4a) is given together with the spectrum of irregular PPy (Figure 4b) for comparison. Two characteristic peaks (at 1.52 eV and ~2.6 eV, respectively) in both absorption spectra indicate the presence of the polarons and bipolarons in the oxidized PPy. The peak at 1.52 eV is attributed to the transition from the bonding to the antibonding polaron state, which corresponds to the doped part of PPy.[25] The peak at ~2.6 eV is associated with the transition from valence band to the antibonding bipolaron state (radical cation/dication level).[26] The red shift of the absorption peak from 2.68 eV (absorption peak of irregular PPy) to 2.61 eV (absorption peak of PPy nanofiber) indicates the existence of hydrogen bonds.[27]

Surface wettability of the PPy film is important for practical applications, particularly promoting immobilization of the hydrophilic probe molecule in sensors and enhancing the penetration and diffusion ability through the film in energy storage/conversion systems.[28] In the water contact angle measurement the water droplet (1 μL) spread fast over the surface and soon was imbibed in the PPy nanofiber film. The film shows a superhydrophilic property with a contact angle close to zero. It is known that both topographic structure and chemical composition contribute to the wettability of a solid surface.[29] The surface of the PPy nanofiber network exhibits homogeneous nanostructure and roughness in the submicrometer scale, resulting in a great enhancement of hydrophilicity. In addition, the incorporation of $HPO_4^{2-}/H_2PO_4^-$ anions in PPy nanofiber film can also contribute to the hydrophilicity improvement through their hydrophilic functional groups.

Conclusion

In summary, we demonstrate a template-free electrochemical synthesis route to fabricate a superhydrophilic PPy nanofiber networked film in an aqueous solution by using PBS. A mechanism for the nanofiber formation in an aqueous solution without assistance of any "hard" and "soft" template is proposed, in which the presence of the hydrogen bonding between phosphate and Py oligomers is essential to produce the 1D nanofiber structure, and the electrostatic interactions between ion dopant and Py oligomers lead to an irregular nanostructure. Additionally, the electrochemical reaction rate plays a significant role in the formation of the 1D ordered nanostructure. The proposed mechanism is not only in good agreement with the characterization of various PPy films formed with different synthetic conditions but also further confirmed by low angle XRD and UV−visible absorption spectra. The developed method opens a way to *in situ* synthesize PPy nanofiber network in an aqueous solution, and has potential to be developed as a universal method for template-free synthesis of 1D nanostructures. Particularly, the superhydrophilic property of the conductive nanofiber network enables its great potential applications in biosensors, energy systems and drug delivery devices.

Acknowledgment. This work is financially supported by Center of Advanced Bionanosystems of Nanyang Technological University in Singapore.

Supporting Information Available: FESEM images of PPy prepared under different experimental conditions. The synthetic parameters that were adjusted include PBS concentration, pH value, Py concentration, ClO_4^- concentration and oxidation potential. This material is available free of charge via the Internet at http://pubs.acs.org.

References and Notes

(1) (a) Aleshin, A. N. *Adv. Mater.* **2006**, *18* (1), 17–27. (b) Huang, Y.; Duan, X. F.; Cui, Y.; Lauhon, L. J.; Kim, K. H.; Lieber, C. M. *Science* **2001**, *294* (5545), 1313–1317.

(2) Wanekaya, A. K.; Bangar, M. A.; Yun, M.; Chen, W.; Myung, N. V.; Mulchandani, A. *J. Phys. Chem. C* **2007**, *111* (13), 5218–5221.

(3) (a) Yang, H. H.; Zhang, S. Q.; Tan, F.; Zhuang, Z. X.; Wang, X. R. *J. Am. Chem. Soc.* **2005**, *127* (5), 1378–1379. (b) Ramanathan, K.; Bangar, M. A.; Yun, M.; Chen, W.; Myung, N. V.; Mulchandani, A. *J. Am. Chem. Soc.* **2005**, *127* (2), 496–497.

(4) Berdichevsky, Y.; Lo, Y. H. *Adv. Mater.* **2006**, *18* (1), 122–125.

(5) Wu, C. G.; Bein, T. *Science* **1994**, *264* (5166), 1757–1759.

(6) Xiao, R.; Cho, S. I.; Liu, R.; Lee, S. B. *J. Am. Chem. Soc.* **2007**, *129* (14), 4483–4489.

(7) Martin, C. R. *Adv. Mater.* **1991**, *3* (9), 457–459.

(8) (a) Zhang, Z. M.; Wei, Z. X.; Wan, M. X. *Macromolecules* **2002**, *35* (15), 5937–5942. (b) Wu, A. M.; Kolla, H.; Manohar, S. K. *Macromolecules* **2005**, *38* (19), 7873–7875. (c) Woodson, M.; Liu, J. *J. Am. Chem. Soc.* **2006**, *128* (11), 3760–3763. (d) Ma, X. F.; Li, G.; Wang, M.; Cheng, Y. N.; Bai, R.; Chen, H. Z. *Chem. Eur. J.* **2006**, *12* (12), 3254–3260. (e) Dai, T. Y.; Yang, X. M.; Lu, Y. *Nanotechnology* **2006**, *17* (12), 3028–3034.

(9) Yang, Y. S.; Wan, M. X. *J. Mater. Chem.* **2001**, *11* (8), 2022–2027.

(10) (a) Ma, Y. F.; Zhang, J. M.; Zhang, G. J.; He, H. X. *J. Am. Chem. Soc.* **2004**, *126* (22), 7097–7101. (b) Dong, L. Q.; Hollis, T.; Fishwick, S.; Connolly, B. A.; Wright, N. G.; Horrocks, B. R.; Houlton, A. *Chem. Eur. J.* **2007**, *13* (3), 822–828.

(11) Bocharova, V.; Kiriy, A.; Vinzelberg, H.; Mönch, I.; Stamm, M. *Angew. Chem., Int. Ed.* **2005**, *44* (39), 6391–6394.

(12) Chiou, N. R.; Epstein, A. J. *Adv. Mater.* **2005**, *17* (13), 1679.

(13) Huang, J. X.; Kaner, R. B. *J. Am. Chem. Soc.* **2004**, *126* (3), 851–855.

(14) (a) Li, C. M.; Sun, C. Q.; Chen, W.; Pan, L. *Surf. Coat. Technol.* **2005**, *198* (1−3), 474–477. (b) Cui, X. Q.; Li, C. M.; Zang, J. F.; Zhou, Q.; Gan, Y.; Bao, H. F.; Guo, J.; Lee, V. S.; Moochhala, S. M. *J. Phys. Chem. C* **2007**, *111*, 2025–2031. (c) Dong, H.; Li, C. M.; Chen, W.; Zhou, Q.; Zeng, Z. X.; Luong, J. H. T. *Anal. Chem.* **2006**, *78* (21), 7424–7431. (d) Hu, W. H.; Li, C. M.; Cui, X. Q.; Dong, H.; Zhou, Q. *Langmuir* **2007**, *23* (5), 2761–2767.

(15) Zhou, Q.; Li, C. M.; Li, J.; Cui, X. Q.; Gervasio, D. *J. Phys. Chem. C* **2007**, *111* (30), 11216–11222.

(16) Cai, Z. H.; Lei, J. T.; Liang, W. B.; Menon, V.; Martin, C. R. *Chem. Mater.* **1991**, *3* (5), 960–967.

(17) (a) Zhong, W. B.; Liu, S. M.; Chen, X. H.; Wang, Y. X.; Yang, W. T. *Macromolecules* **2006**, *39* (9), 3224–3230. (b) He, C.; Yang, C. H.; Li, Y. F. *Synth. Met.* **2003**, *139* (2), 539–545.

(18) Koo, Y. K.; Kim, B. H.; Park, D. H.; Joo, J. *Mol. Cryst. Liq. Cryst.* **2004**, *425*, 333–338.

(19) (a) Huang, J. X.; Kaner, R. B. *Angew. Chem., Int. Ed.* **2004**, *43* (43), 5817–5821. (b) Martin, C. R. *Science* **1994**, *266* (5193), 1961–1966.

(20) Liang, L.; Liu, J.; Windisch, C. F.; Exarhos, G. J.; Lin, Y. H. *Angew. Chem., Int. Ed.* **2002**, *41* (19), 3665–3668.

(21) (a) Tamm, T.; Tamm, J.; Karelson, M. *Synth. Met.* **2005**, *149* (1), 47–52. (b) Matsumoto, A.; Kitajima, T.; Tsutsumi, K. *Langmuir* **1999**, *15*, 7626–7631.

(22) (a) Hoeben, F. J. M.; Jonkheijm, P.; Meijer, E. W.; Schenning, A. *Chem. Rev.* **2005**, *105* (4), 1491–1546. (b) Hunter, C. A.; Sanders, J. K. M. *J. Am. Chem. Soc.* **1990**, *112* (14), 5525–5534. (c) Prins, L. J.; Reinhoudt, D. N.; Timmerman, P. *Angew. Chem., Int. Ed.* **2001**, *40* (13), 2382–2426. (d) Reinhoudt, D. N.; Crego-Calama, M. *Science* **2002**, *295* (5564), 2403–2407.

(23) Alvarez-Romero, G. A.; Garfias-Garcia, E.; Ramirez-Silva, M. T.; Galan-Vidal, C.; Romero-Romo, M.; Palomar-Pardave, M. *Appl. Surf. Sci.* **2006**, *252* (16), 5783–5792.

(24) (a) Zhang, L. J.; Long, Y. Z.; Chen, Z. J.; Wan, M. X. *Adv. Funct. Mater.* **2004**, *14* (7), 693–698. (b) Zhang, L. J.; Wan, M. X. *Adv. Funct. Mater.* **2003**, *13* (10), 815–820.

(25) Furukawa, Y.; Tazawa, S.; Fujii, Y.; Harada, I. *Synth. Met.* **1988**, *24* (4), 329–341.

(26) Genies, E. M.; Pernaut, J. M. *J. Electroanal. Chem.* **1985**, *191* (1), 111–126.

(27) Jin, J.; Iyoda, T.; Cao, C. S.; Song, Y. L.; Jiang, L.; Li, T. J.; Zhu, D. B. *Angew. Chem., Int. Ed.* **2001**, *40* (11), 2135–2138.

(28) (a) Zhu, Y.; Hu, D.; Wan, M. X.; Jiang, L.; Wei, Y. *Adv. Mater.* **2007**, *19* (16), 2092–2096, Chen, G.; Wang. (b) Zhang, L.; Hui, R.; Zhang, J. J. *Adv. Funct. Mater.* **2007**, *17* (11), 1844–1848.

(29) Sun, T. L.; Feng, L.; Gao, X. F.; Jiang, L. *Acc. Chem. Res.* **2005**, *38* (8), 644–652.

MA801345K